VIMS Articles

Virginia Institute of Marine Science

Environmental controls on pteropod biogeography along the Western Antarctic Peninsula

Patrica S. Thibodeau
Virginia Institute of Marine Science

Deborah K. Steinberg
Virginia Institute of Marine Science

SE Stammerjohn

C Hauri

Recommended Citation

Thibodeau, Patrica S.; Steinberg, Deborah K.; Stammerjohn, SE; and Hauri, C, Environmental controls on pteropod biogeography along the Western Antarctic Peninsula (2019). *Limnology and Oceanography*, 64, S240-s256.
10.1002/lno.11041

Environmental controls on pteropod biogeography along the Western Antarctic Peninsula

P. S. Thibodeau, [1]* D. K. Steinberg, [1] S. E. Stammerjohn,[2] C. Hauri[3]
[1]Virginia Institute of Marine Science, College of William & Mary, Gloucester Point, Virginia
[2]Institute of Arctic and Alpine Research, University of Colorado at Boulder, Boulder, Colorado
[3]International Arctic Research Center, University of Alaska Fairbanks, Fairbanks, Alaska

Abstract

Pteropods are abundant zooplankton in the Western Antarctic Peninsula (WAP) and important grazers of phytoplankton and prey for higher trophic levels. We analyzed long-term (1993–2017) trends in summer (January–February) abundance of WAP pteropods in relation to environmental controls (sea ice, sea surface temperature, climate indices, phytoplankton biomass and productivity, and carbonate chemistry) and interspecies dynamics using general linear models. There was no overall directional trend in abundance of thecosomes, *Limacina helicina antarctica* and *Clio pyramidata,* throughout the entire WAP, although *L. antarctica* abundance increased in the slope region and *C. pyramidata* abundance increased in the South. High *L. antarctica* abundance was strongly tied to a negative Multivariate El Niño Southern Oscillation Index the previous year. *C. pyramidata* abundance was best explained by early sea ice retreat 1-yr prior. Abundance of the gymnosome species, *Clione antarctica* and *Spongiobranchaea australis*, increased over the time series, particularly in the slope region. Gymnosome abundance was positively influenced by abundance of their prey, *L. antarctica,* during the same season, and late sea ice advance 2-yr prior. These trends indicate a shorter ice season promotes longer periods of open water in spring/summer favoring all pteropod species. Weak relationships were found between pteropod abundance and carbonate chemistry, and no long-term trend in carbonate parameters was detected. These factors indicate ocean acidification is not presently influencing WAP pteropod abundance. Pteropods are responsive to the considerable environmental variability on both temporal and spatial scales—key for predicting future effects of climate change on regional carbon cycling and plankton trophic interactions.

Pteropods (pelagic snails) are ubiquitous holoplanktonic zooplankton that are an important link between primary producers and higher trophic organisms, major contributors to organic and inorganic carbon flux, and key indicators of ecosystem health (Foster et al. 1987; Pakhomov et al. 1996; Giraldo et al. 2011; Manno et al. 2017). Both thecosome and gymnosome pteropods (shelled and nonshelled, respectively) are common components in the diets of carnivorous zooplankton, fish (such as cod, salmon, and herring), and sea birds in many regions including the Antarctic and Pacific Northwest (Hopkins 1987; Pakhomov et al. 1996; Hunt et al. 2008; Giraldo et al. 2011; Sturdevant et al. 2012). All types of pteropods influence carbon cycling via their grazing and predation and subsequent fecal pellet production (Lalli and Gilmer 1989;

Bernard and Froneman 2003; Hunt et al. 2008; Bernard et al. 2012). Additionally, thecosomes produce mucous feeding webs which aggregate and export particulate organic matter (Gilmer and Harbison 1986; Manno et al. 2017). Thecosome pteropods, and larval gymnosomes–which shed their shells during metamorphosis into adults, also contribute to carbon cycling through the sinking and dissolution of their aragonitic shells, which results in the release of carbonate ions thus influencing the inorganic carbon pump (Lalli and Gilmer 1989; Howard et al. 2011; Manno et al. 2017). It is estimated that global pteropod biomass is approximately 500 Tg C and that thecosomes contribute between 20% and 40% of the global carbonate production and at least 12% of the total carbonate flux (Berner and Honjo 1981; Bednaršek et al. 2012a). The carbonate balance may be disrupted or shifted by ocean acidification (OA), the anthropogenic addition of carbon dioxide to seawater (Doney et al. 2009; Le Quéré et al. 2015). Thecosome pteropods are considered sentinel indicators of OA due to the vulnerability of their aragonitic shells dissolving under increasingly acidic conditions from a changing climate (Orr et al. 2005; Bednaršek et al. 2014; Manno et al. 2017). Other

*Correspondence: psthibodeau@vims.edu

potential effects of climate change on pteropods, particularly in polar oceans, include sea surface temperature (SST) increase and sea ice decline (Mackey et al. 2012; Steinberg et al. 2015; Suprenand et al. 2015a).

The Western Antarctic Peninsula (WAP) is a region of rapid climate change, with annual mean midwinter air temperature increasing 5°C (from −11°C to −6°C) since 1950 (Vaughan et al. 2003; Ducklow et al. 2012b; updated by Stammerjohn, unpubl.). Regional warming and increases in winds led to a long-term decrease in sea ice in the WAP, with a later sea ice advance and earlier retreat, causing a 3 month decrease in the sea ice season since 1990 (Stammerjohn et al. 2012, 2015). Since ~ 2008, the WAP has experienced relatively cooler conditions and longer ice seasons, a short-term trend reversal which has slightly weakened the long-term trends of rapid warming and shorter ice seasons (Schofield et al. 2017). Interannual variability and long-term trends in sea ice advance, retreat, and cover are affected by the southern annular mode (SAM) and El Niño Southern Oscillation (ENSO). Strong La Niña years, in combination with a positive Southern Annual Mode (SAM), produce negative sea level pressure and subsequent anomalously strong winds from the north, particularly in the spring. These winds influence the position of basin-scale water masses and produce earlier (wind-driven) ice-edge retreats, the latter also facilitating warmer ice-free conditions in spring–summer (Stammerjohn et al., 2008b, 2012). In regards to OA, no long-term directional trends were observed in carbonate chemistry parameters based on a 20-yr time series for the WAP, but OA is projected to intensify in the region, in combination with increasing freshwater input, by 2030 (Hauri et al. 2015, 2016). In contrast to the slight weakening of warming trends along the mid-WAP region, a recent analysis indicates a moderate cooling period (-0.47 ± 0.25 decade^{-1}) for the northern WAP region from approximately 1999–2014, which is consistent with the high decadal-scale variability that the Southern Ocean climate naturally exhibits (Turner et al. 2016). Nonetheless, quantitative assessments of observed and projected environmental changes in the Southern Ocean by Gutt et al. (2015) indicate an anthropogenic warming signal in the WAP that will continue to be affected by one or more climate processes in the future.

The thecosome *Limacina helicina antarctica* is one of the most abundant macrozooplankton species along the WAP (Ross et al. 2008; Steinberg et al. 2015) and is an important grazer of phytoplankton in the Southern Ocean (Bernard and Froneman 2003; Bernard et al. 2012). The gymnosome species *Clione antarctica* and *Spongiobranchaea australis* are the only two nonshelled pteropods in the WAP and feed exclusively on local thecosomes, particularly *L. antarctica* (van der Spoel 1967; Boltovskoy 1974; Lalli and Gilmer 1989; van der Spoel and Dadon 1999). Feeding studies of *Clione* spp. indicate they consume a single thecosome within 2–45 min (Conover and Lalli 1972). The population dynamics of these groups are inherently linked through this predator–prey relationship (Seibel and Dierssen 2003). The thecosome *Clio pyramidata* is

the largest of the pteropods present along the WAP, although occurs in relatively smaller abundances (van der Spoel 1967). Both *L. antarctica* and *C. pyramidata* are known to have some of the highest ingestion rates recorded for Southern Ocean zooplankton (Hunt et al. 2008).

Prior studies in the Antarctic and elsewhere indicate a variety of climate and environmental controls on pteropod regional abundance and distribution (Beaugrand et al. 2012; Mackas and Galbraith 2012; Loeb and Santora 2013; Howes et al. 2015; Steinberg et al. 2015; Burridge et al. 2017). In the WAP, strong La Niña years combined with a positive SAM lead to warmer, ice-free waters as described above and favor higher abundances of the thecosome pteropod *L. antarctica* (Ross et al. 2008; Steinberg et al. 2015). Strong La Niña years concomitant with increasingly ice-free regions of the WAP have been suggested to increase *L. antarctica* abundance in the southern WAP (Steinberg et al. 2015). The aragonitic composition of the pteropod calcium carbonate ($CaCO_3$) shell makes them particularly vulnerable to OA through shell dissolution (Orr et al. 2005; Lischka et al. 2011; Bednaršek et al. 2012b; Comeau et al. 2012; Busch et al. 2014). Bednaršek et al. (2014) showed regions along coastal California in which aragonite undersaturation ($[Ca^{2+}][CO_3^{2-}]/K'_{sp} < 1$, where K'_{sp} is the apparent thermodynamic solubility product of $CaCO_3$), a metric for indicating carbonate ion concentration and OA, corresponded to high pteropod shell dissolution. Thus, OA is another environmental factor potentially affecting pteropod abundance. However, warming water temperatures outweighed the effects of OA on pteropod abundance in the Pacific Northwest as shown by time series (1960–2009) analysis, as well as in the Mediterranean (Beaugrand et al. 2012; Howes et al. 2015). While a number of studies document the effect of OA on pteropod physiology and shell condition, the importance of carbonate chemistry as a control on pteropod distribution has not yet been examined in the Southern Ocean.

This study builds upon previous analyses of WAP pteropod biogeography and long-term abundance trends by examining environmental factors that influence abundance of the major pteropod species along the mid-WAP over the last 25-yr (1993–2017). We report long-term trends of all major WAP pteropod taxa in relation to a variety of environmental or ecological controls ranging from SST, to sea ice timing and duration, to predator–prey interactions. This research also represents the first comparison of long-term carbonate chemistry data to pteropod abundance in the Southern Ocean, which could identify potential OA effects. These results will aid in predicting future shifts in pteropods due to effects of climate change and OA, and the consequences of these shifts on the role of pteropods in biogeochemical cycling and energy transfer in this polar region.

Methods

Study region

The Palmer, Antarctica Long Term Ecological Research (PAL LTER) study region is located along the middle of the WAP,

bounded by Palmer Station, Anvers Island (64.77°S, 64.05°W) in the north and Charcot Island (69.45°S, 75.15°W) approximately 700 km to the south, and from the Peninsula coast to the continental slope 200 km offshore (Ducklow et al., 2007, 2012*b*) (Fig. 1). Sampling of grid stations occurred annually during PAL LTER summer research cruises (approximately 01 January to 10 February) aboard the MV *Polar Duke* (1993–1997) and ARSV *Laurence M. Gould* (1998 to present). Grid lines are spaced 100 km apart perpendicular to the WAP, with stations spaced 20 km apart along each grid line (Waters and Smith 1992). Before 2009, zooplankton were collected from all stations from lines 600 to 200. Line 100 was sampled in 2007 and 2008 but regular sampling of the far south

stations (lines 100, 000, and −100) was not incorporated into the sampling grid until 2009. The expansion of the gridlines further south enabled the PAL LTER to include a region with longer sea ice duration and extent but resulted in decreased sampling intensity per line throughout the grid (from ~ 10 sampling stations per line pre-2009 to ~ 3 thereafter). For most analyses, either the entire grid (Full Grid) was considered, or the grid was divided into latitudinal subregions based on hydrographic and sea ice conditions as in Steinberg et al. (2015): "North" (lines 600, 500, and 400), "South" (lines 300 and 200), and "Far South" (100, 000, and −100) (Fig. 1). For the general linear model (GLM) and other analyses as appropriate, the "South" and "Far South" data were combined
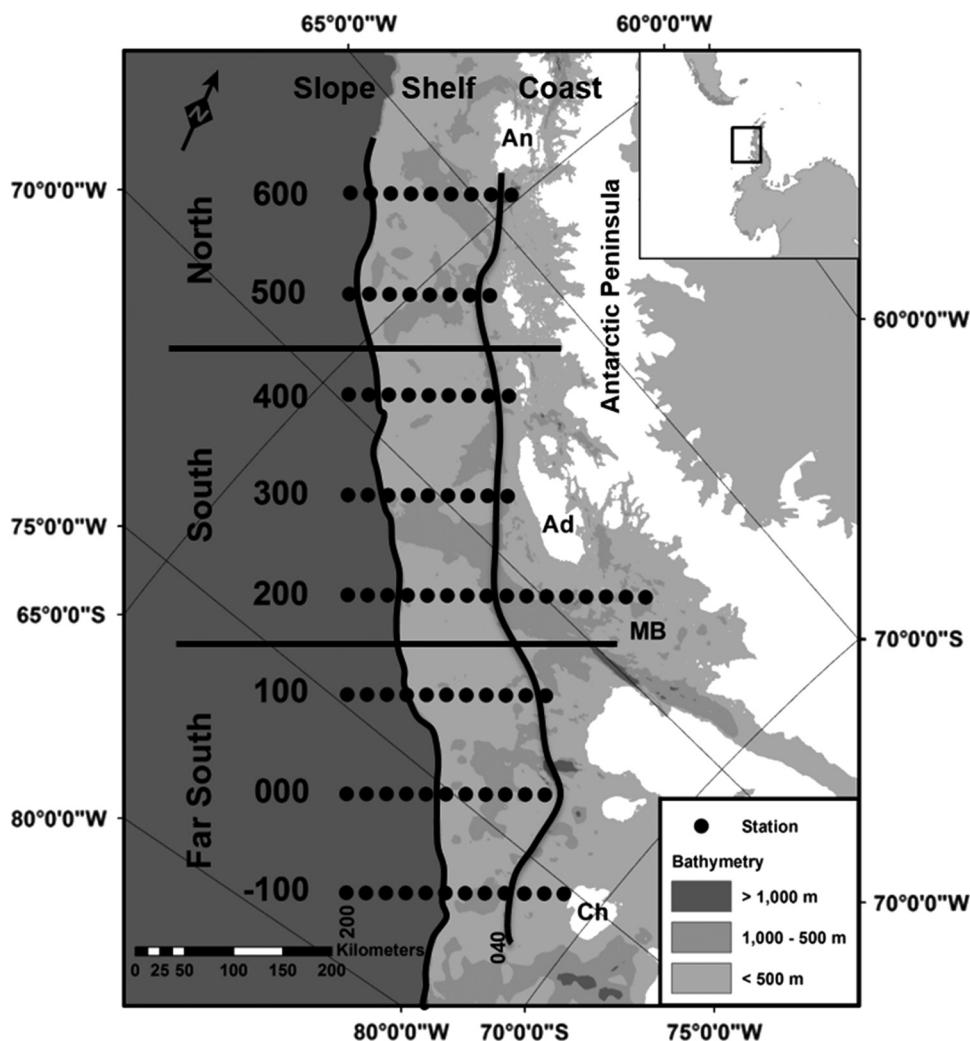

Fig. 1. Map of PAL LTER study region. Study region (highlighted in box) relative to the Antarctic continent. Shades of gray illustrate bathymetry, with light gray indicating the continental shelf and dark gray the continental slope and abyssal plain. Shelf break is represented by light/dark gray interface near 1000 m, extending down to 3000 m (Ducklow et al., 2012*b*). The continental shelf is roughly 200 km wide and 430 m deep on average. Canyons that cut into the shelf can reach up to 1000 m deep. PAL LTER grid lines are numbered from 600 to −100, with the far slope (200) and shelf stations indicated for reference (Waters and Smith 1992). Grid lines are distanced 100 km apart and individual stations for a given grid line are 20 km apart. Horizontal lines delineate the "North," "South," and "Far South" subregions. Vertical lines indicate the coastal, shelf, and slope subregions. All region divisions are based on hydrographic and sea ice conditions (Martinson et al. 2008; Stammerjohn et al. 2008*a*). An, Anvers Island, the location of Palmer Station; MB, Marguerite Bay; Ad, Adelaide Island; Ch, Charcot Island.

into "South+" (lines 300, 200, 100, 000, and −100), and the coast-shelf-slope (on to offshore) gradient as defined by Martinson et al. (2008) was included. To assign regions for samples not collected at a standard grid station, sampling locations were rounded to the nearest standard 100 km grid line and 20 km grid station.

Pteropod collection and sampling

Pteropod and all other macrozooplankton collection were performed with a 2-m square frame Metro net (700-μm mesh), towed obliquely to depths of ~ 120 m (Ross et al. 2008; Steinberg et al. 2015). Net depth was determined real time with a depth sensor attached to the bottom of a conducting wire and verified with a temperature-depth recorder. A General Oceanics flow meter oriented in the center of the net mouth was used to calculate volume filtered. Pteropods, in addition to the rest of the whole catch, were sorted by species, subspecies on board, and the abundance and total biovolume (of fresh, unpreserved animals) of each species was determined. We analyzed data for the four major pteropod species identified in the time series: thecosomes *L. antarctica* and *C. pyramidata* and gymnosomes *C. antarctica* and *S. australis* (van der Spoel and Dadon 1999; Ross et al. 2008). Abundances of the latter two species were combined (hereafter "gymnosomes"), as earlier in the time series (1993–2008) *S. australis* and *C. antarctica* were only identified to order level rather than to species. Identification of *C. pyramidata* did not begin until 2004, therefore we refer to long-term trends in *C. pyramidata* abundance from 2004 to 2017 only. We present our analyses only as abundance data, as trends in biovolume closely mirrored that of abundance for all pteropods and some biovolume data were not available prior to 2009 (see Supporting Information Fig. 1).

Effects of day vs. night sampling (i.e., potentially higher densities in surface waters at night due to diel vertical migration-DVM) on results were examined using the approach described in Steinberg et al. (2015) and summarized here. Sun elevation at the time and location of each tow (Meeus 1998) was determined with night defined at a sun elevation of ≤ −0.833°. Night densities (*n* = 250 tows) were compared to day (*n* = 1056 tows) (Wilcoxon test, $p < 0.05$), and the mean night : day ratio (N:D) was determined for each pteropod species with significantly higher night density than day. These species included *L. antarctica* (N:D = 1.4) and gymnosomes (N:D = 1.4) but not *C. pyramidata* (likely due to low abundance of *C. pyramidata* overall reducing their chance of being sampled in night tows). To allow direct inter-comparison of all tows, night abundance values were corrected (reduced) by dividing them by the N:D ratio to calculate a diel-corrected abundance. Other studies have used diel abundance corrections in their time series analyses (e.g., Mackas et al. 2001; Atkinson et al. 2008; Ross et al. 2014).

Environmental parameters and climate indices

Considered environmental parameters affecting pteropod abundance include: phytoplankton biomass (chlorophyll *a* [Chl *a*]) and primary production (PP), carbonate chemistry, SST, sea ice cover, and climate indices. Chl *a*, PP, dissolved inorganic carbon (DIC), and total alkalinity (TA) were measured at each station from samples taken within the euphotic zone, as described in Vernet et al. (2008), Ducklow et al. (2012*a*, 2012*b*), Hauri et al. (2015), and Steinberg et al. (2015). Discrete measurements of Chl *a* were integrated to 100 m and PP to the deepest PP measurement (i.e., bottom of the euphotic zone). Carbonate chemistry variables including calculated pH measured on the total scale and saturation state for aragonite (Ω_{ar}) were determined from averaged values of DIC, TA, and temperature, salinity, phosphate, silicate, and pressure collected from the euphotic zone using the CO2SYS MATLAB version (Van Heuven et al. 2011) and as described in Hauri et al. (2015). No TA data were collected in 2003–2004. SST was determined by the NOAA optimal interpolation (OI) SST analysis (version OI.v2) using in situ and satellite SSTs as well as SSTs simulated by sea ice cover (Reynolds et al. 2002). These data are located at http://iridl.ldeo. columbia.edu/SOURCES/.NOAA/.NCEP/.EMC/.CMB/.GLOBAL/. Reyn_SmithOIv2/. SST was averaged over the entire PAL LTER grid and for the subregions such that 'North' was within 200 km south and west of Anvers Island, 'South' was within 200 km south and west of Avian Island, and 'Far South' was within 200 km west of Adelaide Island (Fig. 1). Monthly data were used to determine annual and seasonal means as follows: spring (September–October–November), summer (December–January–February), and fall (March–April–May). There were no winter SST data due to ice cover. SST concomitant with the time of zooplankton sampling in January was also estimated via OI.

Sea ice parameters included extent, area, duration, date of advance, date of retreat, and number of ice days. These data were derived from satellite imagery (Scanning Multichannel Microwave Radiometer and Special Sensor Microwave/Imager; SMMR-SSM/I) as described in Stammerjohn et al. (2008*a*). SMMR-SSM/I sea ice concentration data were from the Earth Observing System Distributed Active Archive Center at the National Snow and Ice Data Center, University of Colorado (http://nsidc.org). "Sea ice extent" is the total area within the sea ice edge, and "sea ice area" is the ocean area covered by sea ice that excludes open areas inside the ice edge (both in km^2). Annual "ice season duration" is the number of days between when sea ice first appears in the fall (advance) and last appears in the spring (retreat). "Sea ice days" are the number of days between the day of advance and retreat when ice concentration remained above 15% (Stammerjohn et al. 2008*a*). Spatial averages of these sea ice parameters (described above) were determined for the entire PAL LTER study grid as well as for the same subregions as described for SST above. All the above data

in the analyses are available at: http://oceaninformatics.ucsd.edu/datazoo/data/palterlter/datasets.

The relationship between pteropod taxon abundance and climate indices known to influence the pelagic Antarctic Peninsula region was analyzed (Ross et al. 2008; Stammerjohn et al. 2008*b*; Loeb and Santora 2013; Saba et al. 2014; Steinberg et al. 2015). These indices include the ENSO indicator based on SST (referred to as the multivariate ENSO index [MEI]; http://www.esrl.noaa.gov/psd/people/klaus.wolterlter/MEI/) and the SAM (http://www.antarctica.ac.uk/met/gjma/sam.html) index based on sea level pressure. These climate indices are seasonally adjusted (e.g., Hurrell 1995). Annual climate indices were averaged over the entire PAL LTER grid and for the subregions as described for SST and sea ice above.

In order to test relationships between pteropod taxon abundance and environmental forcing concurrent with the time of our summer (January/February) cruise sampling we lagged the data with 0-, 1-, and 2-yr lags. The "summer" sampling season spans two calendar years (e.g., December 2016, January 2017, and February 2017) when sampling zooplankton as well as measurements for Chl *a*, PP, carbonate chemistry, SST, and climate indices. Therefore, the calendar year for the end of the summer sampling season was used to define the lag for these parameters. For example, a significant relationship between *L. antarctica* abundance in January 2017 and a 1-yr lag in SST would indicate that variation in *L. antarctica* abundance was affected by summer SST in 2016 (mean of December 2015, January 2016, and February 2016). In contrast, a 1-yr lag in sea ice extent would indicate that sea ice extent in the winter of 2016 affected *L. antarctica* abundance the following January 2017.

Anomaly calculations

Anomalies are a useful unitless ratio to transform data for comparison of interannual trends across a variety of plankton and other hydrographic variables, each with different measurement units and sampling frequencies (Wiebe et al. 2016). The abundance anomaly (A'_y) for each pteropod taxon and year in the time series was calculated using the following formula:

$$A'_y = log_{10}[\overline{A_y}/\overline{A}]$$

where $\overline{A_y}$ is the mean abundance for year *y*, and $\overline{A}$ is the mean of the yearly means (O'Brien et al. 2011; Steinberg et al. 2015; Wiebe et al. 2016). Anomalies were calculated for the entire grid and separately for different subregions. The relative magnitude of each annual anomaly was only compared with others of the same pteropod taxon within the same subregion. Annual summer-time anomalies for Chl *a*, PP, carbonate chemistry, SST, and annual anomalies for sea ice parameters were calculated in the same way as pteropod taxon abundance anomalies. Climate indices are already in anomaly form and do not have subregional anomalies.

Regional comparison

A three-way ANOVA, with data in annual anomaly form, was used to determine differences in regional abundance for each pteropod taxon, as well as broad-scale differences in taxon abundance between the first (1993–2005) and second (2006–2017) halves of the time series (North/South+ × coast/shelf/slope × early/late time series). To assess if the recent long-term cooling effect along the WAP since 2008 has affected pteropod abundances, a three-way ANOVA was performed partitioning the time series into the first (1993–2001), second (2002–2010), and third (2011–2017) periods (Schofield et al. 2017). Multiple comparisons were adjusted with a Tukey correction. Note *C. pyramidata* was not recorded as a separate category in the time series until 2004.

Comparison of environmental parameters, climate indices, and species interactions

GLMs, with data in annual anomaly form for the Full Grid, were developed to explore the effects of covariates on abundance of different pteropod taxa. The covariates included annual Chl *a*, PP, SST, carbonate chemistry, the six ice variables, two climate indices as well as *L. antarctica* abundance anomaly (for gymnosome model only). The data met all assumptions of multiple linear regression including homogeneity of variance, normally distributed data, fixed predictors, and no multicollinearity among predictors. Covariates from the GLMs were assessed for outlying and influential observations and normality of residuals. Positive autocorrelation was tested with the Durbin-Watson test (Neter et al. 1996). Chosen covariates in the models were based on a priori hypotheses about how those covariates affect pteropod abundance. Climate indices (MEI and SAM) and sea ice parameters were chosen as covariates in models because Steinberg et al. (2015) found strong La Niña years, in combination with increasingly ice-free regions of the WAP, corresponded with long-term increases in *L. antarctica* abundance in the southern WAP. Chl *a* and PP were used in model building because Loeb and Santora (2013) suggest higher *L. antarctica* abundance in the North Peninsula region resulted from increased PP. Carbonate chemistry parameters were used to develop models because many studies have indicated pteropods are particularly susceptible to OA conditions leading to shell dissolution and metabolism suppression (Bednaršek et al. 2012*b*; Maas et al. 2012). The final best fitting model for each taxon was identified based on the highest adjusted R^2 value (Quinn and Keough 2002). Individual regressions were determined for environmental variables, and climate indices (annual anomaly form) against abundance of each pteropod taxon. Comparisons between pteropod taxa were also analyzed with individual regression. Significance for all statistical analyses was determined at $\alpha = 0.05$. All analyses were performed in R statistical framework version 3.2.4 (R Core Team 2013).

Results

Climatology of pteropod abundance and distribution

L. antarctica was the most abundant pteropod in the WAP region followed by the gymnosomes (mean of 63 and 1.5 ind. 1000 m^{-3}, respectively) and then *C. pyramidata* (0.3 ind. 1000 m^{-3}; Table 1). Maximum abundances for all pteropod taxa were 2–3 orders of magnitude higher than the mean (Table 1). The highest abundance of *L. antarctica* and gymnosomes occurred in the slope region (Table 1; Fig. 2). *L. antarctica* mean abundance was similar North to South+ but progressively increased from coast to shelf to slope (Table 1; Fig. 2a). On average, the highest abundance for any species and subregion was for *L. antarctica* in the North slope ($p < 0.001$, ANOVA; Table 1). The gymnosomes followed a similar distribution pattern to *L. antarctica,* with highest mean abundance in the slope region ($p < 0.001$, ANOVA; Table 1) and no North to South+ gradient change in abundance (Table 1; Fig. 2b). Although both *L. antarctica* and gymnosome abundance progressively increased from coast to slope, there were some coastal stations with high mean abundance along the 500 line and in the Far South region (Fig. 2a,b). *C. pyramidata* was the least abundant pteropod with consistently low densities throughout the WAP (Table 1). In contrast to *L. antarctica* and gymnosomes, *C. pyramidata* did not exhibit a strong coast to slope density gradient but instead an increase in abundance from North to South+ ($p = 0.009$, ANOVA; Table 1; Fig. 2c) with highest densities along the 200 and 300 sampling grid lines (Fig. 2c).

Long-term changes in pteropod abundance and distribution

Overall, throughout the WAP region (Full Grid), thecosomes *L. antarctica* and *C. pyramidata* abundance oscillated throughout the time series with no long-term directional change ($p > 0.05$, ANOVA), while gymnosome abundance anomalies increased ($p < 0.001$, ANOVA) linearly over 1993–2017 ($p = 0.007$, $r^2 = 0.27$; Fig. 3). There was no significant difference in thecosome species abundances between the mid (2002–2010) to late (2011–2017) periods of the time series in relation to the recent increase in sea ice since 2008 ($p > 0.05$, ANOVA). Gymnosomes exhibited a decrease in mean abundance from the mid to late periods that was significant ($p = 0.03$, ANOVA). High positive anomalies of *L. antarctica* usually occurred every ~ 6–7 yr, although spectral analysis revealed this apparent periodicity was not significant ($p > 0.05$, Bartlett's Kolmogorov–Smirnov statistic; Fuller 1996). The most negative *L. antarctica* anomaly occurred in 1998 and the most positive in 2011 (Fig. 3a). A marked switch from negative to positive anomalies occurred in 2008 for *L. antarctica* and gymnosomes (Fig. 3a,b), and 2008 was also the most positive anomaly year for *C. pyramidata* (Fig. 3c). The switch was particularly marked for gymnosomes—with the only prior positive anomaly before this time in 2002—and abundance anomalies remained positive through the second half of the time series with one exception (2016). *C. pyramidata* abundance anomalies were largely positive from 2006 to 2012, negative from 2013 to 2016, and switched back to positive in 2017 (Fig. 3c).

Abundance anomalies for all three taxa in the latitudinal subregions along the North to South gradient of the WAP largely mirrored those of the Full Grid, but some differences between subregions were apparent. Oscillating periods of negative and positive anomalies of *L. antarctica* were most prevalent in the North, and a period of strong positive anomalies from 2008 to 2012 occurred in the South (Fig. 4a). In 2007 a strong negative *L. antarctica* anomaly occurred in the Far South that was not reflected in the North or South; in contrast, a strong positive anomaly in 2011 occurred in all three latitudinal subregions. The long-term increase in gymnosomes was significant in each subregion (North: $p = 0.002$, $r^2 = 0.3$;

Table 1. Pteropod abundances along the WAP for the entire time series (1993–2017). Mean abundance ± 1 standard deviation (SD) and maximum (max). The minimum abundance for all species was zero. The Full Grid (all stations) and subregions are shown. There are two latitudinal subregions (North and South+; each of which include coast, shelf, and slope stations) and three longitudinal subregions (coast, shelf, and slope; each of which include North and South+ stations). Full Grid (lines −100 to 600), North (lines 400–600), and South+ (lines −100 to 300). For coast, shelf, and slope designations see Fig. 1. Data include both day and night tows, with night data corrected for DVM patterns to allow for direct comparison (*see* Methods). Values are calculated across the entire data set (i.e., annual means were not calculated first and then averaged for all years). The number of observations, *n* (in parentheses), is shown for each subregion.

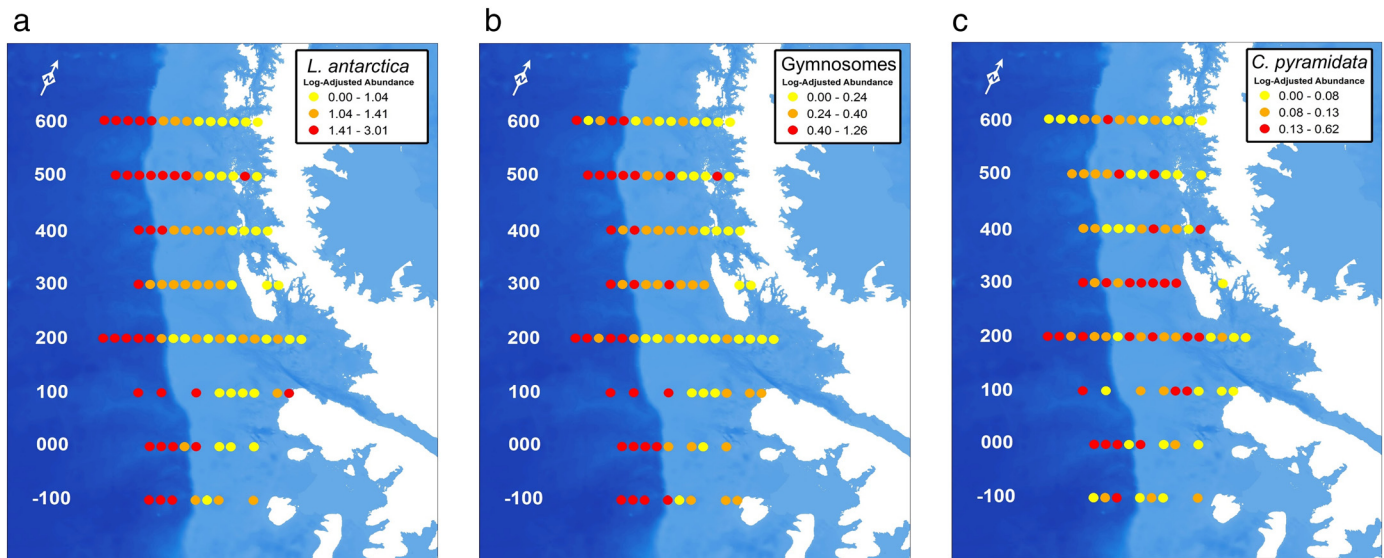|	Abundance by region (individuals 1000 m^{-3})																
	Full grid			**North**			**South+**			**Coast**			**Shelf**			**Slope**	
Taxon	Mean SD	Max		Mean SD	Max		Mean SD	Max		Mean SD	Max		Mean SD	Max		Mean SD	Max
L. antarctica	63 ± 162	4038		58 ± 107	932		69 ± 209	4038		32 ± 105	1410		64 ± 193	4038		99 ± 129	1010
Gymnosomes	1.5 ± 3.4	38		1.6 ± 3.4	38		1.5 ± 3.4	28		0.6 ± 1.4	15.2		1.5 ± 2.9	27		2.8 ± 5	38
C. pyramidata	0.3 ± 0.6	5.9		0.2 ± 0.5	3.8		0.3 ± 0.7	5.9		0.2 ± 0.5	2.3		0.4 ± 0.7	5.9		0.3 ± 0.5	3.1
n for each region	(661–1275)			(297–679)			(364–596)			(266–443)			(261–582)			(172–288)	

Fig. 2. Pteropod climatology for the WAP. Log-adjusted mean abundances (individuals m^{-3}) of **(a)** *L. antarctica* (1993–2017), **(b)** Gymnosomes (1993–2017), and **(c)** *C. pyramidata* (2004–2017). Contours are calculated based on quantiles for the data range of each species separately.

South: $p = 0.001$, $r^2 = 0.34$; Far South: $p = 0.02$, $r^2 = 0.37$; Fig. 4b). While gymnosome anomalies in the North and South subregions switched from negative to positive in 2008, the switch occurred 3-yr later in the Far South (Fig. 4b). Some differences between subregions in patterns of *C. pyramidata* abundance anomalies occurred, including at the end of the time series with a switch in the North between a period of positive and negative anomalies (2011–2017) vs. in the South where anomalies remained negative after 2012 (Fig. 4c).

Pteropod abundance increases were strongest along the WAP slope as well as in the South region. *L. antarctica* abundance anomalies oscillated between positive and negative in the coast and shelf, and significantly increased over time in the slope region ($p = 0.04$, $r^2 = 0.12$) (Fig. 5a). The largest positive anomaly in *L. antarctica* occurred in 2011 in all regions, and the strongest negative anomaly was in 1998 in the shelf and slope. A significant long-term increase in gymnosomes occurred in the shelf and slope regions (shelf: $p = 0.01$, $r^2 = 0.18$, slope: $p < 0.01$, $r^2 = 0.63$) but not the coast (Fig. 5b). However, the switch from negative to positive anomalies in 2008 described above was apparent in all three subregions (Fig. 5b). Strong positive gymnosome anomalies occurred consistently throughout the slope region (2008–2015) with the strongest positive anomaly in 2009. *C. pyramidata* followed a similar trend to *L. antarctica* with an oscillating pattern in abundance anomalies, although there were no long-term directional trends in any region (Fig. 5c).

Environmental and climate influences on pteropod abundance

The best fitting GLM indicated that the MEI index (1-yr lag) was the best, and only statistically significant, parameter for predicting *L. antarctica* variability (Table 2). SAM (1-yr lag),

SST (1-yr lag), sea ice advance (2-yr lag), and aragonite saturation (1-yr lag) were also important parameters in the model, but not statistically significant. We note that sea ice advance (1-yr lag) was negatively correlated with MEI (1-yr lag) ($r^2 = 0.52$, Pearson) and therefore could not be included in the same model (see also below). The best fitting model for gymnosomes indicated *L. antarctica* abundance (no lag) and later sea ice advance (2-yr lag) as important, statistically significant, parameters in predicting gymnosome abundance (Table 2). TA (1-yr lag) was also important but not a statistically significant parameter. Model results for *C. pyramidata* indicated sea ice retreat (1-yr lag) was the most significant parameter. Sea ice extent (2-yr lag) and SAM (2-yr lag) also had a significant effect on *C. pyramidata* abundance while aragonite saturation (1-yr lag) did not (Table 2).

Individual regression relationships between predictors of pteropod abundance identified by the GLM or examples of others that were significant are shown in Fig. 6. Sea ice was an important predictor, with later sea ice advance leading to significantly higher gymnosome abundance (2-yr later) but not to significantly higher *L. antarctica* abundance (Fig. 6a). Years of early sea ice retreat also led to significantly higher *C. pyramidata* abundance the following summer (Fig. 6b). *L. antarctica* abundance was significantly negatively related to MEI (Fig. 6c) and positively related to SST (Fig. 6d) the year prior. The best fitting GLMs did not identify any carbonate chemistry parameters as significant in explaining pteropod abundance, although they accounted for some of the variance in all the models of best fit (Table 2). *C. pyramidata* abundance increased linearly with TA (Fig. 7a). Aragonite saturation, a potentially strong predictor for shelled pteropods in relation to OA, was not significantly related to *L. antarctica* or *C. pyramidata* abundance (Fig. 7b,c).
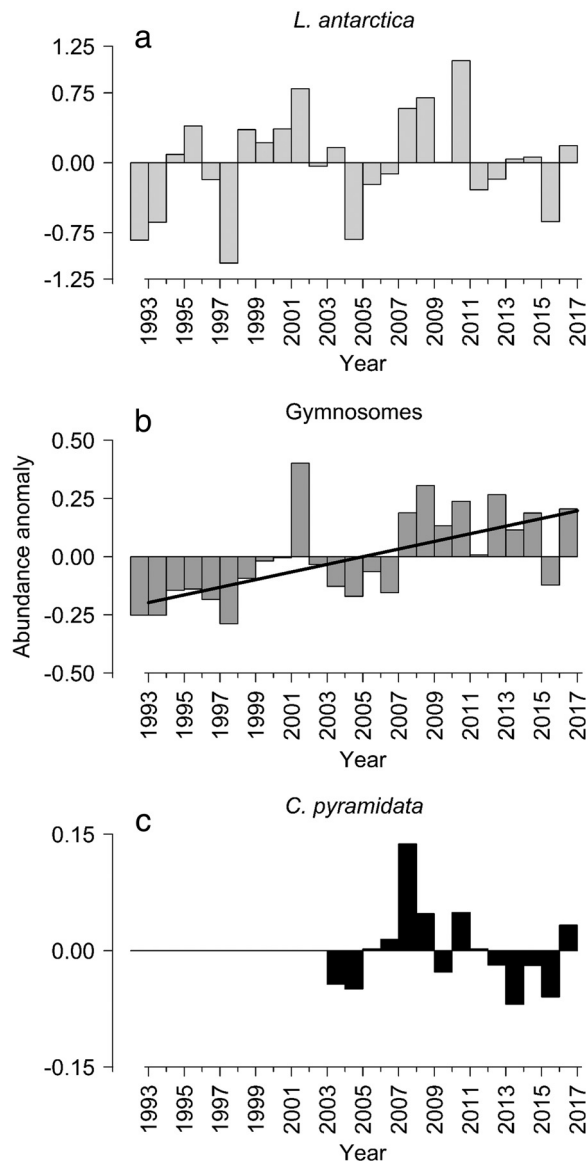
Fig. 3. Annual pteropod abundance anomalies for the full WAP grid. **(a)** *L. antarctica*, **(b)** Gymnosomes, and **(c)** *C. pyramidata*. Anomalies were calculated separately for each species therefore relative height of bars should only be compared with others of the same species. Regression line indicates significant linear relationship (Gymnosomes: *p* = 0.007, r^2 = 0.27).

Pteropod predator–prey and other interspecific dynamics

As gymnosomes, *C. antarctica* and *S. australis,* are known to feed almost exclusively on *L. antarctica* (van der Spoel 1967; Boltovskoy 1974; Lalli and Gilmer 1989; van der Spoel and Dadon 1999) simple linear regressions were performed for the Full Grid with 0-, 1-, and 2-yr lags between predator and prey (i.e., gymnosome abundance anomalies in 2017 were regressed against *L. antarctica* and *C. pyramidata* abundance anomalies in 2017, 2016, and 2015). There was a significant positive linear relationship between *L. antarctica* vs. gymnosome abundance anomalies in the same year (no lag) (Fig. 8a). There

were no significant relationships between these two taxa using *L. antarctica* lags of 1- and 2-yr behind gymnosome abundance, nor between gymnosome and *C. pyramidata* abundance. There was a significant positive correlation between the two thecosome pteropod species *C. pyramidata* and *L. antarctica* in the same year (Fig. 8b).

Discussion

Long-term and spatial trends in pteropod abundance

Our results show pteropods are increasing in abundance in the WAP confirming observations by Ross et al. (2008) and as projected for other macrozooplankton by Mackey et al. (2012), with gymnosomes increasing throughout the entire region while the thecosomes exhibit subregional increases offshore (*L. antarctica*) and in the South (*C. pyramidata)*. The gymnosomes were the only pteropod taxa to exhibit long-term increases throughout the full WAP, while *L. antarctica* increased in abundance along the slope subregion—particularly in the North, and *C. pyramidata* abundance increased in the South. Our gymnosome results differ from those to the north of the PAL LTER study region, where no long-term increase in the gymnosomes was observed (Loeb and Santora 2013). This increase along the mid-WAP/PAL LTER study region for gymnosomes indicates a southward population increase for these nonshelled pteropod taxa**.** Although Ross et al. (2008) observed a long-term increase in *L. antarctica* abundance in the North shelf subregion of the WAP, ours and other more recent time-series analyses no longer indicate a long-term increase in *L. antarctica* over the shelf (Steinberg et al. 2015). Our study reveals for the first time in the mid-WAP long-term patterns in *C. pyramidata*, with an oscillating trend in abundance and no long-term directional change, similar to the pattern observed north of the PAL LTER study region (Loeb and Santora 2013).

Pteropod abundance in relation to climate indices and sea ice

L. antarctica abundance is primarily controlled by the ENSO cycle, with high abundance following years with a negative MEI (La Niña), a result supported by prior analyses in the Antarctic Peninsula region (Ross et al. 2008; Loeb and Santora 2013; Steinberg et al. 2015). Previous studies emphasize the importance of the 1997 El Niño subsequently leading to a strong La Niña in 1999 and high pteropod abundance (Ross et al. 2008; Loeb and Santora 2013; Steinberg et al. 2015). This period represents an important regime shift within the WAP ecosystem and resulted in a marked switch in pteropod abundance from negative to positive anomalies, particularly for *L. antarctica* (Ross et al. 2008). We find this same trend repeated in 2010, with a strongly negative MEI, followed by a strong positive anomaly for *L. antarctica* in 2011. The year 2010 was also marked by a positive SAM and high SST—conditions that when combined with a negative
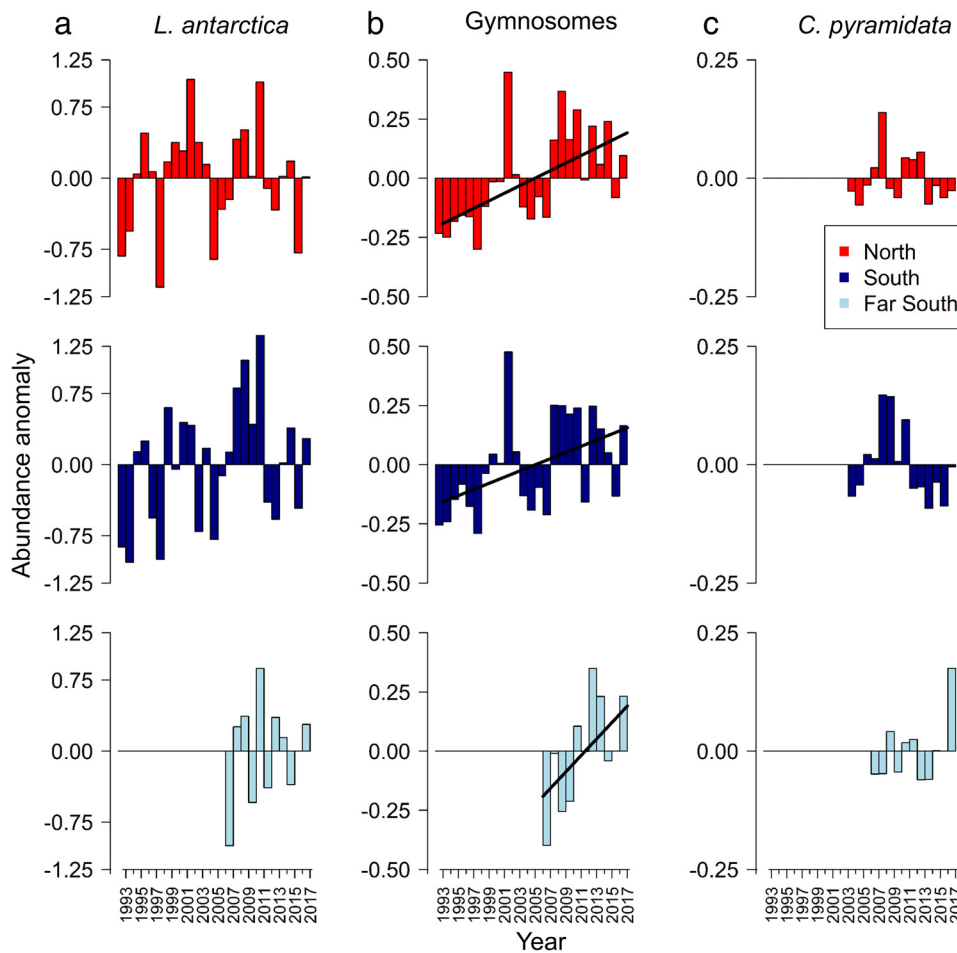
Fig. 4. Annual pteropod abundance anomalies along the WAP latitudinal gradient. **(a)** *L. antarctica*, **(b)** Gymnosomes, and **(c)** *C. pyramidata*. Upper plots represent the "North" subregion (lines 600, 500, and 400), middle plots the "South" (lines 300 and 200), and bottom plots the "Far South" (lines 100, 000, and −100). Anomalies were calculated separately for each species therefore relative height of bars should only be compared with others of the same species and subregion. Regression lines for significant linear relationships are shown, regression statistics are as follows: (b) Gymnosomes—North: $n = 25$, $p = 0.002$, $r^2 = 0.3$; South: $n = 25$, $p = 0.001$, $r^2 = 0.34$; Far South: $n = 11$, $p = 0.026$, $r^2 = 0.37$.

MEI promote shorter ice seasons and warmer, ice-free spring–summers favorable for *L. antarctica* (Steinberg et al. 2015). High positive anomalies of gymnosomes and *C. pyramidata* also followed these low ice, warmer periods, although the trend was not as strong as for *L. antarctica*. Conversely, the year 2015 was characterized by very high sea ice in addition to a strongly positive MEI and negative SST, conditions that resulted in low abundance for all pteropod taxa. These interannual changes support the notion of pteropods as bioindicators given their short generation time (1–3 yr) (Lalli and Gilmer 1989; van der Spoel and Dadon 1999; Bednaršek et al. 2012b) and subsequent ability to respond relatively quickly to changes in the environment (Manno et al. 2017). In the Ross Sea, *L. antarctica* was recently identified to tolerate temperatures far higher (up to 14°C) than experienced in their current summer environment (~ 0°C) (Hoshijima et al. 2017). This thermal tolerance may explain *L. antarctica*'s positive relationship with SST and its

expansion into ice-free, warmer waters. In addition, positive pteropod anomalies continued to occur post-2008, suggesting pteropods have been unaffected by the overall rebound in sea ice in the WAP since that time (Schofield et al. 2017).

Our study indicates that gymnosome abundance is most strongly controlled by *L. antarctica* abundance during the same summer season, which is described below (*see Pteropod interspecific dynamics*). Late sea ice advance (2-yr prior), indicative of a shorter ice season, was also an important parameter and most likely led to the high gymnosome abundance anomaly in 2002 as sea ice advance anomaly was strongly positive in 2000. Low TA accounted for variance in the gymnosome model of best fit and may be related to increased summer sea ice melt and subsequent freshening decreasing TA (Hauri et al. 2015). The marked switch from negative to positive abundance anomalies for gymnosomes in 2008 also corresponded with a period of strong positive anomalies in ice advance starting in 2007. A study in the PAL LTER region in
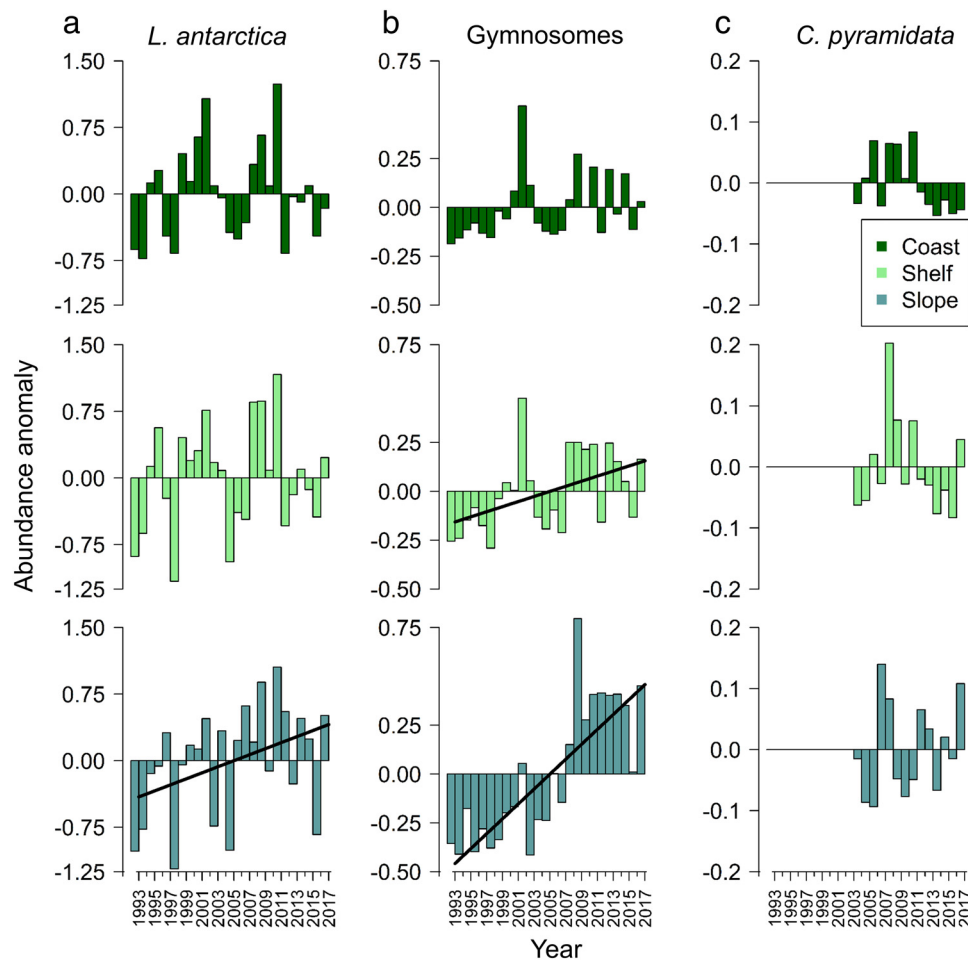
Fig. 5. Annual pteropod abundance anomalies for the WAP coast-shelf-slope gradient. **(a)** *L. antarctica*, **(b)** Gymnosomes, and **(c)** *C. pyramidata*. *See* Fig. 1 for delineation of coast/shelf/slope subregions. Anomalies were calculated separately for each species therefore relative height of bars should only be compared with others of the same species and subregion. Regression lines for significant linear relationships are shown, and regression statistics are as follows: (a) *L. antarctica*—slope: $n = 25$, $p = 0.04$, $r^2 = 0.12$; (b) Gymnosomes—shelf: $n = 25$, $p = 0.01$, $r^2 = 0.18$; slope: $n = 25$, $p < 0.01$, $r^2 = 0.63$.

late summer (March–April 2010) found warmer waters favored the gymnosome *S. australis,* which were more abundant in warm waters influenced by Upper Circumpolar Deep Water (UCDW) upwelling near the shelf break, suggesting they may be better physiologically adapted to warmer waters. In contrast, *C. antarctica* was more abundant in cold waters associated with the coast (Suprenand et al. 2015*a*). Gymnosome species were recorded in warmer waters (~ 2°C) in the WAP indicating their ability to tolerate increasingly subantarctic conditions (Suprenand et al. 2015*b*). To the north of the PAL LTER region, high gymnosome abundance corresponded most strongly to a negative MEI in the fall and positive SAM during the summer season (Loeb and Santora 2013), although sea ice and *L. antarctica* abundance were not directly included in that study. While SST was not an important factor in our analysis, it is worth noting that the 2-yr of high gymnosome abundance (2002 and 2008) were both also strongly positive SST years. Later sea ice advance may explain long-term increases

in gymnosomes offshore and elsewhere as they are exposed to more open water later in the season and potentially more time to feed. Gymnosomes are considered physiologic generalists and therefore, tolerant of changes in the ocean environment, particularly with advection of warm water masses in increasingly open water regions of the WAP (Lalli and Gilmer 1989; Suprenand et al. 2015*a*). Later sea ice advance 2-yr prior may also support gymnosome recruitment. While less is known about the life cycle for Antarctic gymnosomes, their Arctic counterpart, *Clione limacina*, has a 2-yr life cycle (Böer et al. 2006), therefore later sea ice advance and subsequently more open water may promote high gymnosome recruitment and high adult abundance 2-yr later. Thus, we propose that *L. antarctica* abundance most strongly influences gymnosome abundance, while late sea ice advance and warmer waters offshore have led to their increase.

C. pyramidata was most strongly controlled by sea ice retreat the year prior, with early retreat preceding the highest

Table 2. GLM results addressing the effect of environmental, climate, and food on WAP pteropod abundance. Explanatory variables and statistical scores obtained from the best model, identified by the highest R^2 value, among multiple linear regression analyses. Climate indices: SAM, southern annular mode; MEI, multivariate ENSO index. Test statistics include R^2, p values, sample size (n) for the overall model with data presented in anomaly form, the coefficient (slope) for the regression equation, and the standard error (SE) associated with the model coefficient.

Parameter	n	Coefficient	SE	p
L. antarctica (R^2 adjusted = 0.58, p = 0.001)	25			
MEI (1-yr lag)		−0.34461	0.11752	= **0.009**
SST (1-yr lag)		2.98994	1.68443	= 0.09
SAM (1-yr lag)		0.29470	0.18505	= 0.13
Sea ice advance (2-yr lag)		2.04309	1.71175	= 0.25
Aragonite saturation Ω_{ar} (1-yr lag)		−0.73107	1.81501	= 0.69
Gymnosomes (R^2 adjusted = 0.67, p < 0.001)	25			
L. antarctica abundance (0-yr lag)		0.21132	0.05044	< **0.001**
Sea ice advance (2-yr lag)		1.41962	0.50461	= **0.01**
TA (1-yr lag)		−6.59681	3.87079	= 0.1
C. pyramidata (R^2 adjusted = 0.81, p = 0.002)	14			
Sea ice retreat (1-yr lag)		−1.87401	0.00865	< **0.001**
Sea ice extent (2-yr lag)		0.39672	0.28831	= **0.01**
SAM (2-yr lag)		0.06483	0.02442	= **0.03**
Aragonite saturation Ω_{ar} (1-yr lag)		−0.23906	0.19968	= 0.27

C. pyramidata abundance anomaly of the time series in 2008. Other factors, such as positive SAM (2-yr lag) and positive sea ice extent (2-yr lag) were also significant, and in combination with early sea ice retreat, aligned to promote the high 2008 abundance anomaly. Correspondingly, a late sea ice retreat from 2013 to 2016 was closely associated with low *C. pyramidata* abundance during this same period. Lack of physiological data for *C. pyramidata* in the Southern Ocean makes it difficult to mechanistically link their response to these changes in their environment (Hunt et al. 2008). We posit that like *L. antarctica*, earlier sea ice retreat promotes the expansion of *C. pyramidata* further South and could explain their increased abundance in this subregion. Therefore, early sea ice retreat is the most important covariate for predicting *C. pyramidata* abundance in the future.

Carbonate chemistry

Our study represents the first in the Antarctic to relate long-term trends in carbonate chemistry seawater conditions to *L. antarctica* abundance, addressing a gap in data observations connecting biological sampling and processes that measure water carbonate chemistry as emphasized in Manno et al. (2017). While carbonate chemistry, particularly aragonite saturation, was expected to be an indicator of shelled pteropod abundance, there were no strong trends identified in relation to any pteropod species. High TA was positively related to *C. pyramidata* abundance but was not identified as an important parameter in the GLM. This relationship may potentially result from the indirect effect of increasing primary productivity increasing TA (Wolf-Gladrow et al. 2007).

The results from our analysis support the majority of other long-term analyses around the globe (Ohman et al. 2009; Beaugrand et al. 2012; Howes et al. 2015) indicating that there is no current significant effect of carbonate chemistry parameters (i.e., pH, aragonite saturation, and dissolved carbon dioxide) on *L. antarctica* abundance. In the present case, carbonate chemistry, particularly aragonite saturation, was expected to be an indicator of shelled pteropod abundance as OA has been consistently linked to pteropod shell integrity—particularly in the subantarctic region where *L. antarctica* dissolution was associated with undersaturated aragonitic upwelling deep water (Bednaršek et al. 2012*b*). Currently, the WAP is not significantly undersaturated with respect to aragonite (Hauri et al. 2015) and other environmental factors (e.g., SST and sea ice) are more influential controls of shelled pteropod abundance. The large spatial and temporal variability of pteropods and carbonate parameters in the WAP, and no long-term directional trend in carbonate parameters suggests longer time series may be required to detect significant trends in OA (Henson et al. 2010). Along the WAP, negative MEI strongly increases *L. antarctica* abundance via an earlier ice edge retreat in spring that allows surface waters to warm longer, thus leading to favorable high SST for pteropods. SST is also the dominating factor controlling *Limacina* spp. in more temperate regions (Beaugrand et al. 2012; Howes et al. 2015), as is Chl *a* (Ohman et al. 2009).

While we show, based on our 25-yr time series, that shelled pteropod abundance is not related to carbonate chemistry conditions indicative of OA, a tipping point may soon be
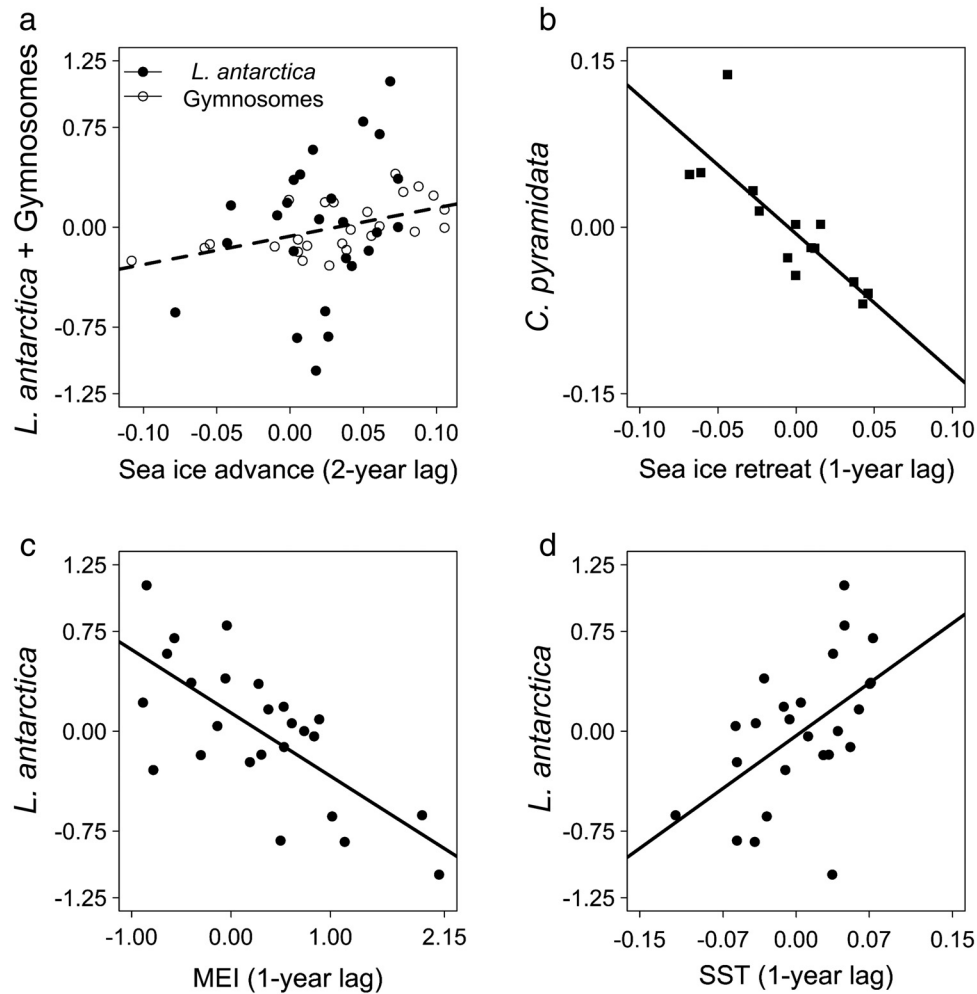
Fig. 6. Effect of environment (sea ice, subdecadal climate oscillations, and SST) on pteropod abundance. **(a)** Sea ice advance vs. *L. antarctica* and Gymnosome abundance. **(b)** Sea ice retreat vs. *C. pyramidata* abundance. **(c)** MEI vs. *L. antarctica* abundance. **(d)** SST vs. *L. antarctica* abundance. Data plotted are annual anomalies for each year of the time series (1993–2017) for the full grid. Sea ice advance is lagged 2-yr behind pteropod abundance (e.g., 2017 pteropod annual anomaly is plotted against 2015 sea ice advance annual anomaly). MEI and SST are lagged 1-yr behind *L. antarctica* abundance (e.g., 2017 *L. antarctica* annual anomaly is plotted against 2016 MEI). Regression lines for significant linear relationships are shown, regression statistics are as follows: (a) sea ice advance vs. *L. antarctica* (filled-circles) and Gymnosomes (empty-circles): $n = 25$, $p = 0.003$, $r^2 = 0.30$ (dashed line); (b) sea ice retreat vs. *C. pyramidata* (squares): $n = 14$, $p = 0.0003$, $r^2 = 0.64$; (c) MEI vs. *L. antarctica* (circles): $n = 25$, $p < 0.001$, $r^2 = 0.47$; (d) SST vs. *L. antarctica* (circles): $n = 25$, $p = 0.006$, $r^2 = 0.25$.

reached as WAP waters are projected to experience prolonged seasons of aragonite undersaturation as early as 2030 (Hauri et al. 2016). The fitness cost of repairing shell dissolution for the thecosomes may not yet influence their abundances possibly because maintenance of other physiologic processes (e.g., respiration and excretion) is more advantageous. In addition, as pteropods were sampled only during the summer as adults, more significant effects of carbonate chemistry on earlier phases in their life cycle may have been missed. This study provides important baseline data for all pteropod taxa in the WAP region and emphasizes the importance of closely monitoring pteropod abundances and carbonate chemistry over seasonal time scales in the future as OA is projected to become more influential.

Pteropod interspecific dynamics

The predator–prey dynamic between the gymnosomes and *L. antarctica* as well as the coupling between *L. antarctica* and *C. pyramidata* indicate the importance in understanding pteropod interspecies relationships when considering pteropod biogeography and their contributions to biogeochemical cycling. Our results indicate that gymnosomes primarily occur offshore following patterns of *L. antarctica* distribution during this same year. *L. antarctica* abundance was the strongest predictor of gymnosome abundance within the current sampling year. While stable *L. antarctica* populations may support current gymnosome abundances, continued increases in gymnosome abundance may eventually limit *L. antarctica* populations. *L. antarctica* and *C. pyramidata* abundance anomalies were
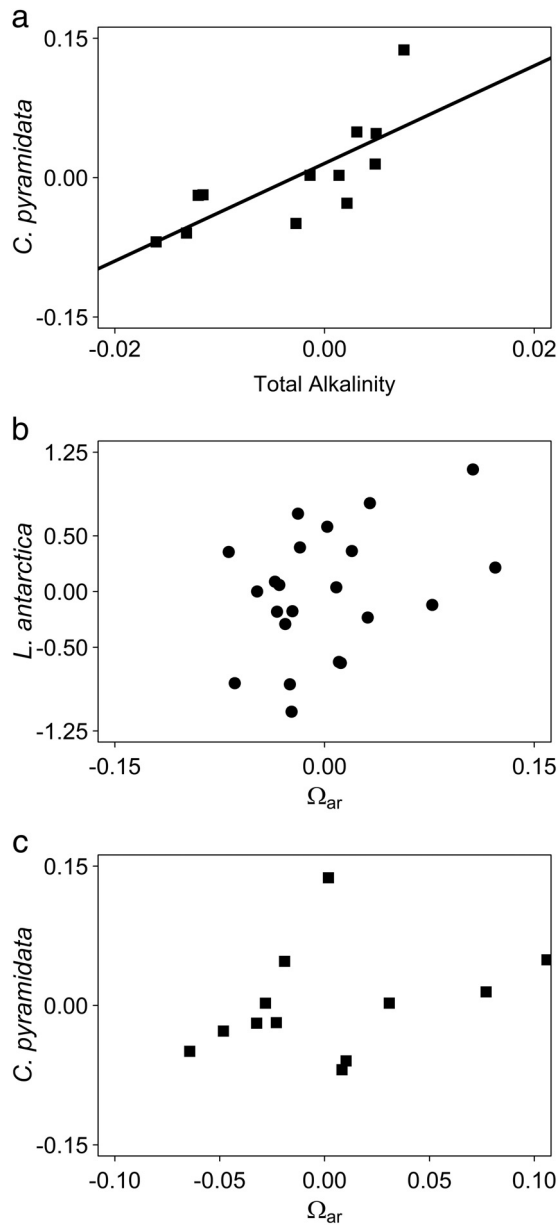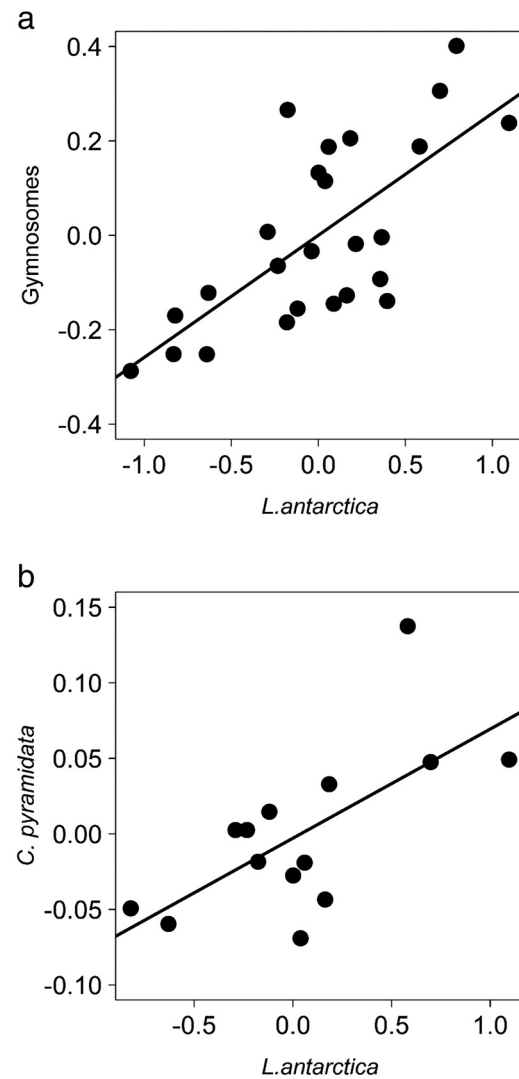
a

b

c

a

b

Fig. 8. Interspecific relationships between pteropod taxa abundance. **(a)** *L. antarctica* vs. Gymnosomes; **(b)** *L. antarctica* vs. *C. pyramidata*. Data are plotted as annual abundance anomalies for each year of the time series (1993–2017, *L. antarctica* and Gymnosome; 2004–2017, *C. pyramidata*) for the full grid. Gymnosomes and *C. pyramidata* values correspond to the same year *L. antarctica* were collected (i.e., no lags). Regression lines for significant linear relationships are shown, regression statistics are as follows: **(a)** *L. antarctica* vs. Gymnosomes: $n = 25$, $p < 0.001$, $r^2 = 0.47$; **(b)** *L. antarctica* vs. *C. pyramidata*: $n = 14$, $p = 0.009$, $r^2 = 0.39$.

Fig. 7. Relationship of thecosome (shelled) pteropod abundance with carbonate chemistry parameters, TA, and aragonite saturation (Ω_{ar}). **(a)** *C. pyramidata* vs. TA. **(b)** *L. antarctica* vs. aragonite saturation. **(c)** *C. pyramidata* vs. aragonite saturation. Data plotted are annual anomalies for each year of the time series (*L. antarctica*: 1993–2017; *C. pyramidata*: 2006–2017) for the full grid. All carbonate chemistry data are lagged 1 yr behind pteropod abundance. No TA data were collected in 2003–2004 (and subsequently Ω_{ar}) and those years were removed from the analysis. Regression lines for significant linear relationships are shown, regression statistics are as follows: (a) *C. pyramidata* (squares) vs. TA: $n = 12$, $p = 0.004$, $r^2 = 0.53$); (b) *L. antarctica* (circles) vs. aragonite saturation: $n = 22$, $p > 0.05$; (c) *C. pyramidata* (squares) vs. aragonite saturation: $n = 12$, $p > 0.05$.

correlated throughout the WAP, which indicates similar environmental conditions, particularly low sea ice, are important controls on Antarctic thecosomes. In addition, none of the

best fitting models explaining pteropod abundance in our study included Chl *a* or PP, in contrast to the tight trophic coupling Seibel and Dierssen (2003) identified between phytoplankton biomass (Chl *a*), *L. antarctica* abundance, and subsequent shifts in *C. antarctica* densities. This may be attributed to differences in sampling scale (localized sampling in McMurdo Sound vs. the large PAL LTER sampling grid) as well as differences between phytoplankton assemblages, with blooms of *Phaeocystis antarctica* nearly dominating in the Ross Sea vs. diatoms often occurring in the WAP (Ducklow et al. 2007; Smith et al. 2007; Schofield

et al. 2017). In addition, the feeding ecology of *L. antarctica* is unknown in the Southern Ocean, therefore PP and Chl *a* may not adequately capture the prey field density preferred by *L. antarctica*.

Conclusions

The effects of climate change along the WAP are changing the biogeography of pteropods, and shifts in their abundance and distribution have important implications for regional carbon cycling and trophic interactions (Steinberg and Landry 2017). Climate oscillations leading to warmer conditions and subsequently low sea ice are important controls on shelled pteropod abundance, with gymnosomes most directly affected by the availability of its prey, *L. antarctica,* as well as later sea ice advance. Thus far pteropods appear to be unaffected by recent sea ice increases in the mid-WAP since 2008, although low pteropod abundances in summer 2016 were clearly reflective of a preceding high ice season. *L. antarctica* is an important grazer in the WAP, and future climate regimes that favor shorter sea ice seasons and warmer, ice-free spring–summer conditions (e.g., La Niñas, positive SAM) may support their increased abundance and grazing pressure. Expansion of *L. antarctica* can sustain higher trophic organisms including planktivorous fish and may promote the increase in gymnosomes as well as other carnivorous zooplankton (e.g., amphipods; Steinberg et al. 2015). In addition, *Limacina* spp. shells can contribute greater than 50% of the carbonate flux in the deep ocean south of the Polar Front (Hunt et al. 2008) and *L. antarctica* and *C. pyramidata* export flux may intensify with their increasing abundance. While OA is not presently a major factor influencing WAP pteropod abundance, OA is projected to grow in importance in the coming decades adding environmental pressure on thecosome shell integrity, physiology and potentially abundance (Bednaršek et al. 2012*b*; Seibel et al. 2012; Manno et al. 2017; Steinberg and Landry 2017). IPCC AR4 model consensus for future warming is strong throughout the Antarctic (Turner et al. 2009). Therefore, the WAP, which is currently experiencing the most rapid warming in the Southern Ocean, represents a natural laboratory in which gradients of environmental influences can act as analogs for predicted future change in other regions of the Antarctic. These regions include ecologically relevant ecosystems such as the Ross Sea Marine Protected Area where *L. antarctica* is extremely abundant. Finally, the relatively short life span of pteropods enables their use as bioindicators not only for future OA but also current environmental conditions, particularly shifts in sea ice and increased SST.

References

Atkinson, A. and others 2008. Oceanic circumpolar habitats of Antarctic krill. Mar. Ecol. Prog. Ser. **362**: 1–23. doi:10.3354/meps07498

Beaugrand, G., A. McQuatters-Gollop, M. Edwards, and E. Goberville. 2012. Long-term responses of North Atlantic calcifying plankton to climate change. Nat. Clim. Chang. **3**: 263–267. doi:10.1038/nclimate1753

Bednaršek, N., G. A. Tarling, S. Fielding, and D. C. E. Bakker. 2012*a*. Population dynamics and biogeochemical significance of *Limacina helicina antarctica* in the Scotia Sea (Southern Ocean). Deep-Sea Res. Part II **59–60**: 105–116. doi:10.1016/j.dsr2.2011.08.003

Bednaršek, N. and others 2012*b*. Extensive dissolution of live pteropods in the Southern Ocean. Nat. Geosci. **5**: 881–885. doi:10.1038/NGEO1635

Bednaršek, N., R. A. Feely, J. C. P. Reum, B. Peterson, J. Menkel, S. R. Alin, and B. Hales. 2014. *Limacina helicina* shell dissolution as an indicator of declining habitat suitability owing to ocean acidification in the California current ecosystem. Proc. Biol. Sci. **281**: 20140123. doi:10.1098/rspb.2014.0123

Bernard, K. S., and P. W. Froneman. 2003. Mesozooplankton community structure and grazing impact in the polar frontal zone of the South Indian Ocean during austral autumn 2002. Polar Biol. **26**: 268–275. doi:10.1007/s00300-002-0472-x

Bernard, K. S., D. K. Steinberg, and O. M. E. Schofield. 2012. Summertime grazing impact of the dominant macrozooplankton off the Western Antarctic Peninsula. Deep-Sea Res. Part I **62**: 111–122. doi:10.1016/j.dsr.2011.12.015

Berner, R. A., and S. Honjo. 1981. Pelagic sedimentation of aragonite : Its geochemical significance. Science **211**: 940–942. doi:10.1126/science.211.4485.940

Böer, M., M. Graeve, and G. Kattner. 2006. Impact of feeding and starvation on the lipid metabolism of the Arctic pteropod *Clione limacina*. J. Exp. Mar. Biol. Ecol. **328**: 98–112. doi:10.1016/j.jembe.2005.07.001

Boltovskoy, D. 1974. Study of surface-shell features in thecosomata (Pteropoda: Mollusca) by means of scanning electron microscopy. Mar. Biol. **27**: 165–172. doi:10.1007/BF00389069

Burridge, A. K., E. Goetze, D. Wall-Palmer, S. L. Le Double, J. Huisman, and K. T. C. A. Peijnenburg. 2017. Diversity and abundance of pteropods and heteropods along a latitudinal gradient across the Atlantic Ocean. Prog. Oceanogr. **158**: 213–223. doi:10.1016/j.pocean.2016.10.001

Busch, D. S., M. Maher, P. Thibodeau, and P. McElhany. 2014. Shell condition and survival of Puget Sound Pteropods are impaired by ocean acidification conditions. PLoS One **9**: e105884. doi:10.1371/journal.pone.0105884

Comeau, S., S. Alliouane, and J. P. Gattuso. 2012. Effects of ocean acidification on overwintering juvenile Arctic pteropods *Limacina helicina*. Mar. Ecol. Prog. Ser. **456**: 279–284. doi:10.3354/meps09696

Conover, R. J., and C. M. Lalli. 1972. Feeding and growth in *Clione limacina* (Phipps), a Pteropod Mollusc. J. Exp. Mar. Biol. Ecol. **9**: 279–302. doi:10.1016/0022-0981(72)90038-X

Doney, S. C., V. J. Fabry, R. a. Feely, and J. a. Kleypas. 2009. Ocean acidification: The other CO_2 problem. Annu. Rev. Mar. Sci. **1**: 169–192. doi:10.1146/annurev.marine.010908.163834

Ducklow, H. W., O. Schofield, M. Vernet, S. Stammerjohn, and M. Erickson. 2012*a*. Multiscale control of bacterial production by phytoplankton dynamics and sea ice along the western Antarctic Peninsula: A regional and decadal investigation. J. Mar. Syst. **98–99**: 26–39. doi:10.1016/j.jmarsys.2012.03.003

Ducklow, H. W. and others 2007. Marine pelagic ecosystems: The West Antarctic Peninsula. Philos. Trans. R. Soc. Lond. Ser. B Biol. Sci. **362**: 67–94. doi:10.1098/rstb.2006.1955

Ducklow, H. W. and others 2012*b*. The marine system of the Western Antarctic Peninsula, p. 121–159. *In* A. D. Rogers, N. M. Johnston, E. J. Murphy, and A. Clarke [eds.], Antarctic ecosystems: An extreme environment in a changing world. Blackwell. doi:10.1002/9781444347241.ch5

Foster, B. A., J. M. Cargill, and J. C. Montgomery. 1987. Planktivory in *Pagothenia borchgrevinki* (Pisces: Nototheniidae) in McMurdo sound. Antarctica Polar Biol. **8**: 49–54. doi:10.1007/BF00297164

Fuller, W. A. 1996. Introduction to statistical time series. John Wiley & Sons.

Gilmer, R. W., and G. R. Harbison. 1986. Morphology and field behavior of pteropod molluscs: Feeding methods in the families Cavoliniidae, Limacinidae and Peraclididae (Gastropoda: Thecosomata). Mar. Biol. **91**: 47–57. doi:10.1007/BF00397570

Giraldo, C., Y. Cherel, C. Vallet, P. Mayzaud, E. Tavernier, M. Moteki, G. Hosie, and P. Koubbi. 2011. Ontogenic changes in the feeding ecology of the early life stages of the Antarctic silverfish (*Pleuragramma antarcticum*) documented by stable isotopes and diet analysis in the Dumont d'Urville Sea (East Antarctica). Polar Sci. **5**: 252–263. doi:10.1016/j.polar.2011.04.004

Gutt, J. and others 2015. The Southern Ocean ecosystem under multiple climate change stresses—an integrated circumpolar assessment. Global Change Biol. **21**: 1434–1453. doi:10.1111/gcb.12794

Hauri, C., S. C. Doney, T. Takahashi, M. Erickson, G. Jiang, and H. W. Ducklow. 2015. Two decades of inorganic carbon dynamics along the Western Antarctic Peninsula. Biogeosci. Discuss. **12**: 6929–6969. doi:10.5194/bgd-12-6929-2015

Hauri, C., T. Friedrich, and A. Timmermann. 2016. Abrupt onset and prolongation of aragonite undersaturation events in the Southern Ocean. Nat. Clim. Change **6**: 172–176. doi:10.1038/nclimate2844

Henson, S. A., J. L. Sarmiento, J. P. Dunne, L. Bopp, I. Lima, S. C. Doney, J. John, and C. Beaulieu. 2010. Detection of anthropogenic climate change in satellite records of ocean chlorophyll and productivity. Biogeosciences **7**: 621–640. doi:10.5194/bg-7-621-2010

Hopkins, T. L. 1987. Midwater food web in McMurdo Sound, Ross Sea, Antarctica. Mar. Biol. **96**: 93–106.

Hoshijima, U., J. M. Wong, and G. E. Hofmann. 2017. Additive effects of pCO2 and temperature on respiration rates of the Antarctic pteropod *Limacina helicina antarctica*. Conserv. Physiol **5**: cox064–cox064. doi:10.1093/conphys/cox064

Howard, W. R., D. Roberts, a. Moy, M. C. M. Lindsay, R. R. Hopcroft, T. W. Trull, and S. G. Bray. 2011. Distribution, abundance and seasonal flux of pteropods in the sub-Antarctic zone. Deep-Sea Res. Part II **58**: 2293–2300. doi:10.1016/j.dsr2.2011.05.031

Howes, E., L. Stemmann, C. Assailly, J. Irisson, M. Dima, J. Bijma, and J. Gattuso. 2015. Pteropod time series from the North Western Mediterranean (1967-2003): Impacts of pH and climate variability. Mar. Ecol. Prog. Ser. **531**: 193–206. doi:10.3354/meps11322

Hunt, B. P. V., E. a. Pakhomov, G. W. Hosie, V. Siegel, P. Ward, and K. Bernard. 2008. Pteropods in Southern Ocean ecosystems. Prog. Oceanogr. **78**: 193–221. doi:10.1016/j.pocean.2008.06.001

Hurrell, J. W. 1995. Decadal trends in the North Atlantic oscillation. Science **269**: 676–679. doi:10.1126/science.269.5224.676

Lalli, C. M., and R. W. Gilmer. 1989. The Thecosomes: Shelled Pteropods, p. 130–145. *In* Pelagic snails. Stanford Univ. Press.

Le Quéré, C. and others 2015. Global carbon budget 2014. Earth Syst. Sci. Data **7**: 47–85. doi:10.5194/essd-7-47-2015

Lischka, S., J. Büdenbender, T. Boxhammer, and U. Riebesell. 2011. Impact of ocean acidification and elevated temperatures on early juveniles of the polar shelled pteropod *Limacina helicina*: Mortality, shell degradation, and shell growth. Biogeosciences **8**: 919–932. doi:10.5194/bg-8-919-2011

Loeb, V. J., and J. A. Santora. 2013. Pteropods and climate off the Antarctic Peninsula. Prog. Oceanogr. **116**: 31–48. doi:10.1016/j.pocean.2013.05.030

Maas, A. E., K. F. Wishner, and B. A. Seibel. 2012. The metabolic response of pteropods to acidification reflects natural CO_2-exposure in oxygen minimum zones. Biogeosciences **9**: 747–757. doi:10.5194/bg-9-747-2012

Mackas, D. L., R. E. Thomson, and M. Galbraith. 2001. Changes in the zooplankton community of the British Columbia continental margin, 1985-1999, and their covariation with oceanographic conditions. Can. J. Fish. Aquat. Sci. **58**: 685–702. doi:10.1139/cjfas-58-4-685

Mackas, D. L., and M. D. Galbraith. 2012. Pteropod time-series from the NE Pacific. ICES J. Mar. Sci. **69**: 448–459. doi:10.1093/icesjms/fsr163

Mackey, A. P., A. Atkinson, S. L. Hill, P. Ward, N. J. Cunningham, N. M. Johnston, and E. J. Murphy. 2012. Antarctic macrozooplankton of the Southwest Atlantic sector and Bellingshausen Sea: Baseline historical distributions

(discovery investigations, 1928-1935) related to temperature and food, with projections for subsequent ocean warming. Deep-Sea Res. Part II **59–60**: 130–146. doi:10.1016/j.dsr2.2011.08.011

Manno, C. and others 2017. Shelled pteropods in peril: Assessing vulnerability in a high CO_2 ocean. Earth-Sci. Rev. **169**: 132–145. doi:10.1016/j.earscirev.2017.04.005

Martinson, D. G., S. E. Stammerjohn, R. a. Iannuzzi, R. C. Smith, and M. Vernet. 2008. Western Antarctic Peninsula physical oceanography and spatio–temporal variability. Deep-Sea Res. Part II **55**: 1964–1987. doi:10.1016/j.dsr2.2008.04.038

Meeus, J. 1998. Astronomical algorithms, 2nd ed. Willmann-Bell.

Neter, J., M. H. Kutner, C. J. Nachtsheim, and W. Li. 1996. Applied linear statistical models. McGraw-Hill Higher Education.

O'Brien, T. D., P. H. Wiebe, and S. J. Hay. 2011 ICES zooplankton status report: 2008/2009. International Council for the Exploration of the Sea.

Ohman, M. D., B. E. Lavaniegos, and A. W. Townsend. 2009. Multi-decadal variations in calcareous holozooplankton in the California current system: Thecosome pteropods, heteropods, and foraminifera. Geophys. Res. Lett. **36**: L18608. doi:10.1029/2009GL039901

Orr, J. C. and others 2005. Anthropogenic Ocean acidification over the twenty-first century and its impact on calcifying organisms. Nature **437**: 681–686. doi:10.1038/nature04095

Pakhomov, E. a., R. Perissinotto, and C. D. McQuaid. 1996. Prey composition and daily rations of myctophid fishes in the Southern Ocean. Mar. Ecol. Prog. Ser. **134**: 1–14. doi:10.3354/meps134001

Quinn, G., and M. Keough. 2002. Experimental design and data analysis for biologists. Cambridge Univ. Press. doi:10.1080/00480169.2002.36305

Reynolds, R. W., N. A. Rayner, T. M. Smith, D. C. Stokes, and W. Wang. 2002. An improved in situ and satellite SST analysis for climate. J. Clim. **15**: 1609–1625. doi:10.1175/1520-0442(2002)015<1609:AIISAS>2.0.CO;2

Ross, R. M., L. B. Quetin, D. G. Martinson, R. A. Iannuzzi, S. E. Stammerjohn, and R. C. Smith. 2008. Palmer LTER: Patterns of distribution of five dominant zooplankton species in the epipelagic zone west of the Antarctic Peninsula, 1993-2004. Deep-Sea Res. Part II **55**: 2086–2105. doi:10.1016/j.dsr2.2008.04.037

Ross, R. M., L. B. Quetin, T. Newberger, C. T. Shaw, J. L. Jones, S. A. Oakes, and K. J. Moore. 2014. Trends, cycles, interannual variability for three pelagic species west of the Antarctic Peninsula 1993-2008. Mar. Ecol. Prog. Ser. **515**: 11–32. doi:10.3354/meps10965

R Core Team, 2013. R: A language and evironment for statistical computing. R Foundation for Statistical Computing, Vienna, Austria. http://www.R-project.org/.

Saba, G. K. and others 2014. Winter and spring controls on the summer food web of the coastal West Antarctic Peninsula. Nat. Commun. **5**: 1–8. doi:10.1038/ncomms5318

Schofield, O. and others 2017. Decadal variability in coastal phytoplankton community composition in a changing West Antarctic Peninsula. Deep-Sea Res. Part I **124**: 42–54. doi:10.1016/j.dsr.2017.04.014

Seibel, B. A., and H. M. Dierssen. 2003. Cascading trophic impacts of reduced biomass in the Ross Sea, Antarctica: Just the tip of the iceberg? Biol. Bull. **205**: 93–97. doi:10.2307/1543229

Seibel, B. A., A. E. Maas, and H. M. Dierssen. 2012. Energetic plasticity underlies a variable response to ocean acidification in the pteropod *Limacina helicina antarctica*. PLoS One **7**: e30464. doi:10.1371/journal.pone.0030464

Smith, W. O., D. G. Ainley, and R. Cattaneo-Vietti. 2007. Trophic interactions within the Ross Sea continental shelf ecosystem. Philos. Trans. R. Soc. Lond. Ser. B Biol. Sci. **362**: 95–111. doi:10.1098/rstb.2006.1956

Stammerjohn, S. E., D. G. Martinson, R. C. Smith, and R. a. Iannuzzi. 2008*a*. Sea ice in the Western Antarctic Peninsula region: Spatio-temporal variability from ecological and climate change perspective. Deep-Sea Res. Part II **55**: 2041–2058.

Stammerjohn, S. E., D. G. Martinson, R. C. Smith, X. Yuan, and D. Rind. 2008*b*. Trends in Antarctic annual sea ice retreat and advance and their relation to El Niño–southern oscillation and southern annular mode variability. J. Geophys. Res. **113**: 1–20. doi:10.1029/2007JC004269

Stammerjohn, S., R. Massom, D. Rind, and D. Martinson. 2012. Regions of rapid sea ice change: An inter-hemispheric seasonal comparison. Geophys. Res. Lett. **39**: 1–8. doi:10.1029/2012GL050874

Stammerjohn, S. E. and others 2015. Seasonal sea ice changes in the Amundsen Sea, Antarctica, over the period of 1979 – 2014. Elem. Sci. **3**: 1–20. doi:10.12952/journal.elementa.000055.

Steinberg, D. K. and others 2015. Long-term (1993–2013) changes in macrozooplankton off the Western Antarctic Peninsula. Deep-Sea Res. Part I **101**: 54–70. doi:10.1016/j.dsr.2015.02.009

Steinberg, D. K., and M. R. Landry. 2017. Zooplankton and the ocean carbon cycle. Annu. Rev. Mar. Sci. **9**: 413–444. doi:10.1146/annurev-marine-010814-015924

Sturdevant, M. V., J. A. Orsi, and E. A. Fergusson. 2012. Diets and trophic linkages of epipelagic fish predators in coastal Southeast Alaska during a period of warm and cold climate years, 1997–2011. Mar. Coast. Fish. **4**: 526–545. doi:10.1080/19425120.2012.694838

Suprenand, P. M., D. L. Jones, and J. J. Torres. 2015*a*. Distribution of gymnosomatous pteropods in western Antarctic Peninsula shelf waters: Influences of Southern Ocean water masses. Polar Rec. (Gr. Brit). **51**: 58–71. doi:10.1017/S003224741300065X

Suprenand, P. M., E. H. Ombres, and J. J. Torres. 2015*b*. Metabolism of gymnosomatous pteropods in waters of the western Antarctic Peninsula shelf during austral fall. Mar. Ecol. **518**: 69–83. doi:10.3354/meps11050

Turner, J., and others. 2009. Antarctic climate change and the environment Published by the Scientific Committee on Antarctic Research. Scott Polar Research Institute, Lensfield Road, Cambridge, UK.

Turner, J. and others 2016. Absence of 21st century warming on Antarctic Peninsula consistent with natural variability. Nature **535**: 411–415. doi:10.1038/nature18645

van der Spoel, S. 1967. Euthecosomata: A group with remarkable developmental stages (Gastropoda, Pteropoda). Printed in the Netherlands by J. Noorduijn en Zoon N.V., Gorinchem.

van der Spoel, S., and J. R. Dadon. 1999. Pteropoda, p. 868–1706. *In* D. Boltovskoy [ed.], South Atlantic zooplankton, v. **1**. Backhuys. doi:10.1097/00004032-199908000-00006

Van Heuven, S., D. Pierrot, J. W. B. Rae, E. Lewis, and D. W. R. Wallace. 2011. CO2SYS v 1.1, MATLAB program developed for CO_2 system calculations. ORNL/CDIAC-105b. Carbon Dioxide Information Analysis Center, Oak Ridge National Laboratory, U.S. Department of Energy. doi:10.1017/CBO9781107415324.004

Vaughan, D. G. and others 2003. Recent rapid regional climate warming on the Antarctic Peninsula. Clim. Change **60**: 243–274. doi:10.1023/A:1026021217991

Vernet, M., D. G. Martinson, R. A. Iannuzzi, S. E. Stammerjohn, W. Kozlowski, K. Sines, R. Smith, and I. Garibotti. 2008. Primary production within the sea ice zone west of the Antarctic Peninsula. Deep-Sea Res. Part II **55**: 2068–2085.

Waters, K. J., and R. C. Smith. 1992. Palmer LTER: A sampling grid for the Palmer LTER program. Antarct. J. **27**: 236–239. doi:10.1017/CBO9781107415324.004

Wiebe, P. H., and others 2016. The ICES working group on zooplankton ecology: Accomplishments of the first 25 years. Prog. Oceanogr. **141**: 179–201. doi:10.1016/j.pocean.2015.12.009

Wolf-Gladrow, D. A., R. E. Zeebe, C. Klaas, A. Körtzinger, and A. G. Dickson. 2007. Total alkalinity: The explicit conservative expression and its application to biogeochemical processes. Mar. Chem. **106**: 287–300. doi:10.1016/j.marchem.2007.01.006

Conflict of Interest

None declared.